

Supporting Information

Sea urchin-like Lanthanum decorated $\text{Ni}_3\text{S}_2@\text{FeOOH}$ for boosting oxygen evolution catalysis in simulated seawater electrolysis

Yaoxia Yang*, Biaobiao Lu, Yu Zhang, RuiRui Zhang, Fuxing Zhou,

Qingtao Wang, Dongfei Sun, Xiaozhong Zhou and Zhiwang Yang

Key Laboratory of Eco-functional Polymer Materials of the Ministry of Education,

Key Laboratory of Polymer Materials of Gansu Province,

College of Chemistry and Chemical Engineering, Northwest Normal University,

Lanzhou 730070, China

*Corresponding author. College of Chemistry and Chemical Engineering, Northwest Normal University, Lanzhou, 730070.

E-mail address: yangyaoxia2007@126.com; yaoxiayang@nwnu.edu.cn (Y-X, Yang).

1. Materials

Ni foam substrate (NF) was supplied by Kunshan Guangjiayuan New Material Co., Ltd. Nickel nitrate hexahydrate ($\text{Ni}(\text{NO}_3)_2 \cdot 6\text{H}_2\text{O}$, $\geq 98.0\%$), Sodium borohydride (NaBH_4 , $\geq 96.0\%$), Urea ($\text{CO}(\text{NH}_2)_2$, $\geq 99.0\%$) and Potassium hydroxide (KOH , $\geq 85.0\%$) were purchased from Sinopharm (China). Lanthanum nitrate hexahydrate ($\text{La}(\text{NO}_3)_3 \cdot 6\text{H}_2\text{O}$, $\geq 99.0\%$), Iron nitrate hexahydrate ($\text{Fe}(\text{NO}_3)_3 \cdot 6\text{H}_2\text{O}$, $\geq 98.0\%$), Ammonium fluoride (NH_4F , $\geq 98.0\%$) were purchased from Aladdin (China). Acetone ($\text{C}_3\text{H}_6\text{O}$, $\geq 99.5\%$) was purchased from Shanghai Experimental Reagent Co., Ltd. Selenium (Se, $\geq 99.99\%$) powder was purchased from Adamas beta (China). Hydrochloric acid (HCl , AR) and Ethanol ($\text{C}_2\text{H}_5\text{OH}$, $\geq 99.7\%$) were purchased from Rionlon Bohua (tianjin) pharmaceutical & Chemical Co., Ltd. Deionized water (18.25Ω).

2. Preparation of LaFeNi/NF

First, the nickel foam was cut into pieces with a size of $1 \times 2 \text{ cm}^2$ and cleaned the nickel foam in 3 M hydrochloric acid solution, acetone solution, absolute ethanol solution, and deionized water respectively for 10 minutes in an ultrasonic cleaner to remove the oxides and impurities on the surface of the nickel foam. Then dissolve 0.4 mmol of $\text{Fe}(\text{NO}_3)_3 \cdot 6\text{H}_2\text{O}$, 0.1 mmol of $\text{Ni}(\text{NO}_3)_2 \cdot 6\text{H}_2\text{O}$, 0.9 mmol of $\text{La}(\text{NO}_3)_3 \cdot 6\text{H}_2\text{O}$, 10 mmol of urea, and 8 mmol of NH_4F in 40 mL of deionized water, stir the mixed solution in a constant-temperature stirrer for 6 hours, transfer the stirred solution and the pre-treated nickel foam into a 100 mL reaction kettle, put the reaction kettle into an oven and keep it at 120°C for 12 hours, and then dry the target sample in an oven at 60°C . To investigate the influence of different La doping amounts on the performance of the

oxygen evolution reaction, a control experiment was set up and samples with La doping amounts of 0 mmol, 0.3 mmol, 0.6 mmol, and 1.2 mmol were prepared using the same method for comparison experiments.

3. Preparation of La-Ni₃S₂@FeOOH/NF

1.96 mmol of thioacetamide was dissolved in 30 mL of deionized water and stirred the solution with a constant-temperature stirrer for 3 hours. The dried precursor sample and the prepared thioacetamide solution put into a 50 mL reaction kettle, and then place it in an oven for a 12-hour solvothermal process at 140 °C to obtain the target sample La-Ni₃S₂@FeOOH/NF. After repeatedly washing the target sample with ethanol solution and deionized water, dry it in an oven at 60 °C overnight. The other precursor comparison samples are also subjected to the same sulfidation process, and the obtained comparison samples are denoted as LaFeNi/NF, 0.3 La-Ni₃S₂@FeOOH /NF, 0.6 La-Ni₃S₂@FeOOH/NF, and 1.2 La-Ni₃S₂@FeOOH/NF respectively.

4. Preparation of RuO₂/NF

10 mg of RuO₂ was dissolved in 950 µL of ethanol and 50 µL of Nafion solution. After ultrasonic treatment for 30 minutes, 200 µL of the suspension was dropped onto 1×2 cm² NF electrodes of the same size and dried at room temperature.

5. Physical characterization

The physical and chemical properties of the catalyst materials were characterized by the following instruments. In order to verify the morphology and elemental composition of the catalyst material, field emission scanning electron microscopy (FE-SEM, Carl

Zeiss Ultra Plus, Germany) and transmission electron microscopy (TEM, JEOL JEM 2100). The elemental mapping of the sample was characterized by energy dispersive X-ray spectroscopy (EDX, Oxford, England) with the equipped Aztec-X-80. Chemical composition and elemental composition were analyzed by X-ray powder diffractometer K (XRD, Rigaku D/Max-2400) with Cu K α radiation source and X-ray photoelectron spectroscopy (XPS) analysis was performed on an analytical instrument (Thermo Scientific K-Alpha) with monochromatic Al K α radiation source. The purpose of this study is to investigate the hydrophilic and aerophobic characteristics of this material, therefore, Contact Angle Analyzer (SL 200KB) was used to test its contact Angle (CA).

6. Electrochemical measurements

The electrochemical testing in this study is conducted using the standard three-electrode system. (CHI760e, CH instrument, Shanghai, China) at room temperature. The standard three-electrode system was used for electrochemical testing. The graphite electrode was used as the counter electrode, and all samples to be tested could be used as self-supported working electrodes. The Hg/HgO electrodes were used as reference electrodes in alkaline media. All the potentials were converted into the reversible hydrogen electrode (vs. RHE) by the Nernst equation:

$$E(\text{RHE}) = E(\text{Hg/HgO}) + 0.059 \text{ pH} + 0.098$$

$$E(\text{RHE}) = E(\text{Ag/AgCl}) + 0.059 \text{ pH} + 0.197$$

La-Ni₃S₂@FeOOH/NF (2×1 cm²) was used as a self-supported working electrode for electrochemical tests in 1.0 M KOH solutions. The OER catalytic activity of each electrode was measured by linear sweep voltammetry (LSV) at a sweep rate of 5 mV

s^{-1} . To analyze the performance of OER, the Tafel plot of the linear region is derived by fitting the Tafel equation ($\eta = a + b \log j$), wherein η represents the overpotential, b signifies the Tafel slope, and j designates the current density. CV curves were obtained by cyclic voltammetry in the sweep rate range of 20 to 120 mV s^{-1} , and the double-layer capacitance (C_{dl}) was calculated. Under the condition of a current density of 10 mA cm^{-2} and a duration of 100 hours, the electrochemical stability is examined using a chronopotentiometry curve. Meanwhile, electrochemical impedance spectroscopy (EIS) measurements were performed in the frequency range of 100 kHz to 0.01 Hz.

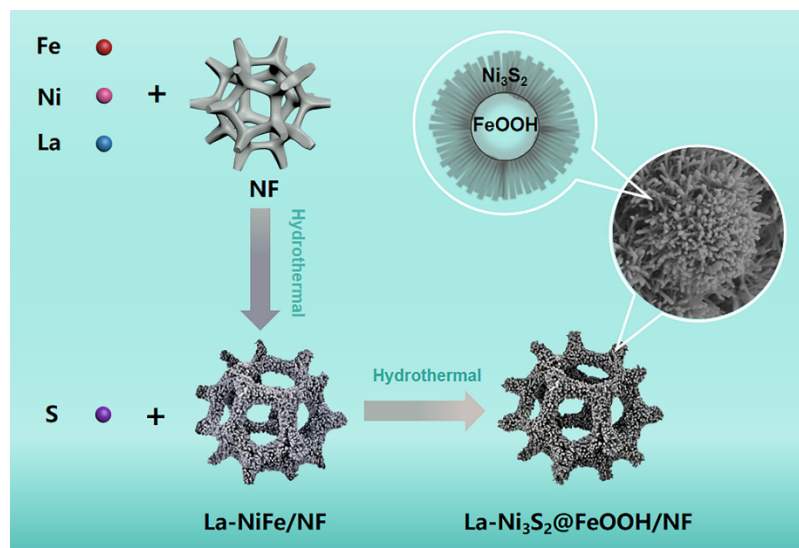


Fig. S1 Diagram of the preparation process of La-Ni₃S₂@FeOOH/NF.

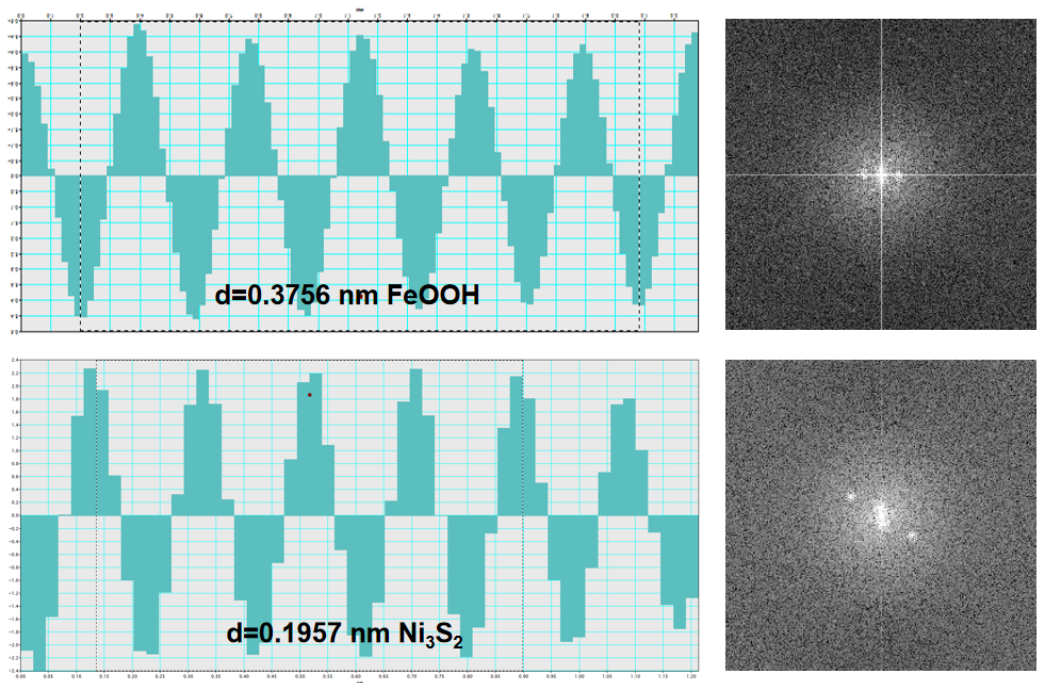


Fig. S2 The lattice spacing measured by the Fourier transform of FeOOH and Ni_3S_2 .

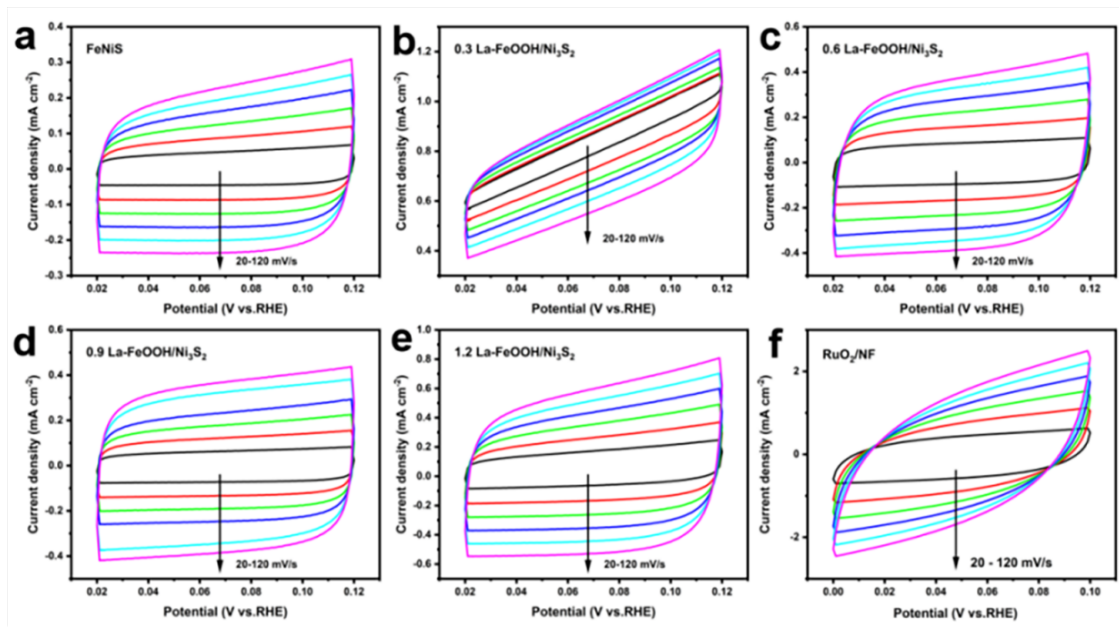


Fig. S3 (a) FeNiS/NF, (b) 0.3 La-Ni₃S₂@FeOOH/NF, (c) 0.6 La-Ni₃S₂@FeOOH/NF, (d) 0.9 La-Ni₃S₂@FeOOH/NF, (e) 1.2 La-Ni₃S₂@FeOOH/NF, and (f) RuO₂/NF CV curves within the non-Faradaic capacitive current range at different scan rates in a simulated seawater environment.

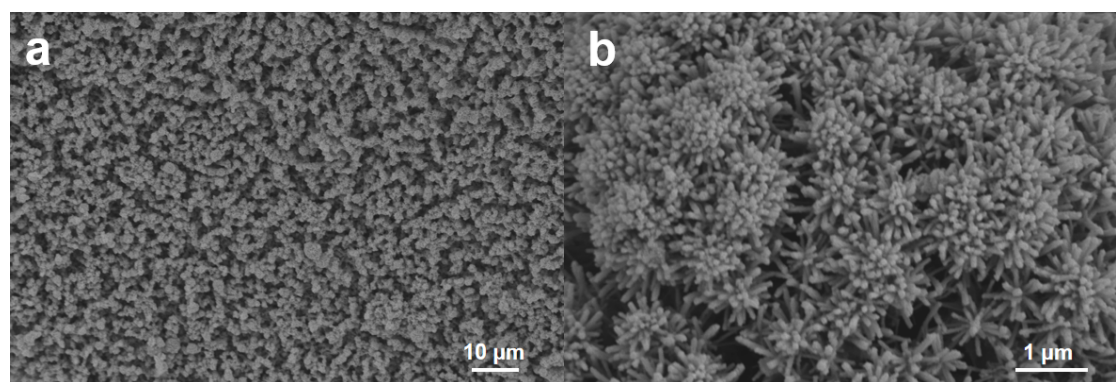


Fig. S4 (a, b) SEM images of La-Ni₃S₂@FeOOH/NF after long OER test.

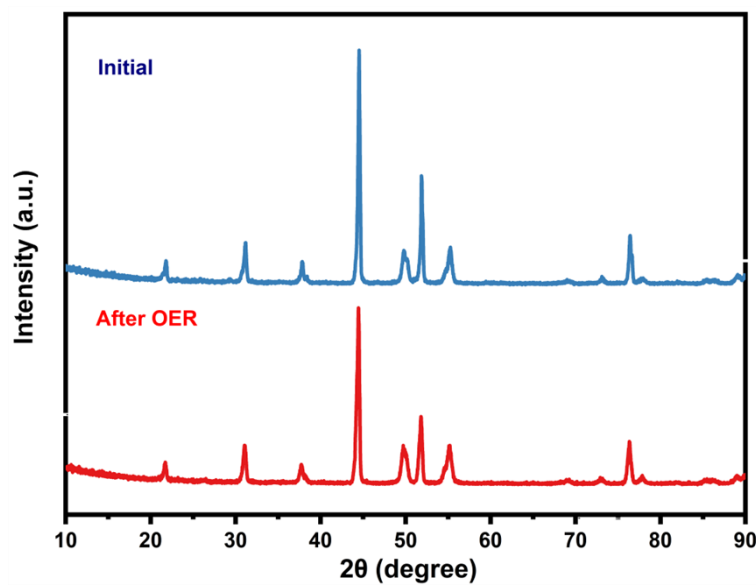


Fig. S5 XRD comparison spectra of La-Ni₃S₂@FeOOH/NF before and after stability test.

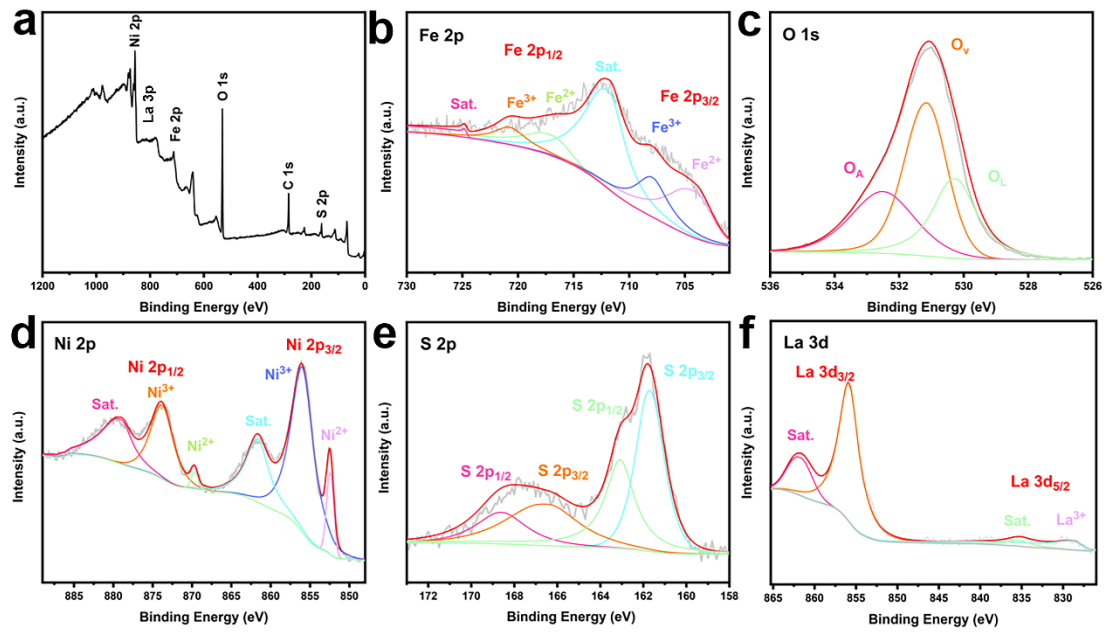


Fig. S6 XPS spectra of La-Ni₃S₂@FeOOH/NF, (a) XPS total spectrum, (b) Fe 2p spectrum, (c) O 1s spectrum, (d) Ni 2p spectrum, (e) S 2p spectrum, (f) La 3d spectrum after stability test in simulated seawater electrolyte solution.

Table S1 OER parameters of various as-prepared catalysts in 1 M KOH+0.5 NaCl.

Catalyst	η_{10} (mV)	Tafel slope (mV dec ⁻¹)	C_{dl} (mF cm ⁻²)
0.9 La-Ni ₃ S ₂ @FeOOH/NF	249	39.13	4.43
FeNiS/NF	284	59.17	1.86
0.3 La-Ni ₃ S ₂ @FeOOH/NF	278	80.20	1.57
0.6 La-Ni ₃ S ₂ @FeOOH/NF	268	79.97	2.91
1.2 La-Ni ₃ S ₂ @FeOOH/NF	269	60.69	3.15

Table S2 Comparison of OER performance of La-Ni₃S₂@FeOOH/NF with other advanced electrocatalysts in Simulated seawater solution medium.

Catalysts	η_{10} (mV)	Tafel slope (mV dec ⁻¹)	References
La-Ni ₃ S ₂ @FeOOH/NF	249	39.13	This work
Co-CoO@C (ZIF67-600Ar/GF)	374	-	[S1]
oct_Cu ₂ O-NF	354	90	[S2]
FTO/NiO	340	-	[S3]
ER-RP/P-SNCF-5	332	-	[S4]
Ni ₃ S ₂ /r-NiS/h-NiS/NF-11h	254	75.11	[S5]
NiMn/Ti-1	386	130	[S6]
Fe-Ni(OH) ₂ /Ni ₃ S ₂ @NF	269	46	[S7]
CoSe/MoSe ₂ /NF	350	-	[S8]
Pb ₂ Ru ₂ O _{7-x}	500	48	[S9]
NiCo ₂ S ₄ /Ni ₃ S ₂	312	-	[S10]
Mo-CoP _x /NF	260	-	[S11]
NiFe-CuCo LDH	220	-	[S12]

Reference

[S1] Sana F, Ghosh A, Ramaprabhu S, ZIF67-derived Co-CoO@C nanocomposites as highly efficient and selective oxygen evolution reaction (OER) catalysts for seawater electrolysis. *Int. J. Hydrogen Energy*, 2024, 49, 780-793.

[S2] Wang H, Ying J, Xiao Y X, Chen J B, Li J H, He Z Z, Yang H J, Yang X Y, Ultrafast synthesis of Cu₂O octahedrons inlaid in Ni foam for efficient alkaline water/seawater electrolysis. *Electrochem. Commun.*, 2022, 134, 107177.

[S3] Juodkazyte J, Sebeka B, Savickaja I, Petrulevi M, Butkut S, Jasulaitien V, Selskis A, Ramanauskas R, Electrolytic splitting of saline water: Durable nickel oxide anode for selective oxygen evolution. *Int. J. Hydrogen Energy*, 2019, 44, 5929-5939.

[S4] Liu F, Hu R, Qiu H, Miao H, Wang Q, Yuan J, Constructing high-activity cobalt-based perovskite hybrid by a top-down phase evolution method for the direct seawater electrolysis anode. *J. Alloys Compd.*, 2022, 913, 165342.

[S5] Liang J, Zhao Z F, Su Z H, Qu W L, Guo R, Li X F, Shang Y C, Multiphase interface coupling of Ni-based sulfide composites for high-current-density oxygen evolution electrocatalysis in alkaline freshwater/simulated seawater/seawater. *Dalton Trans.*, 2024, 53, 15040.

[S6] Sukomol B, Aldona B C, Daina U, Jurate V, Loreta T T, Eugenijus N, Bimetallic Ni-Mn electrocatalysts for stable oxygen evolution reaction in simulated/alkaline seawater and overall performance in the splitting of alkaline seawater. *Coatings*, 2024, 14, 1074.

[S7] Cui B H, Hu Z, Liu C, Liu S, Chen F, Hu S, Zhang J, Zhou W, Deng Y, Qin Z, Wu Z, Chen Y, Cui L, Heterogeneous lamellar-edged Fe-Ni(OH)₂/Ni₃S₂ nanoarray for efficient and stable seawater oxidation. *Nano Res.*, 2021, 14, 1149-1155.

[S8] Sun J, Li J, Li Z, Li C, Ren G, Zhang Z, Meng X, Modulating the electronic structure on cobalt sites by compatible heterojunction fabrication for greatly improved overall water/seawater electrolysis. *ACS Sustain. Chem. Eng.*, 2022, 10, 9980-9990.

[S9] Gayen P, Saha S, Ramani V, Selective seawater splitting using pyrochlore electrocatalyst. *ACS Appl. Energy Mater.* 2020, 3, 3978-3983.

[S10] Gopalakrishnan S, Anandha G B, Harish S, Interface engineering of heterogeneous NiMn layered double hydroxide/vertically aligned NiCo₂S₄ nanosheet as highly efficient hybrid electrocatalyst for overall seawater splitting. *Chemosphere*, 2024, 350, 141016.

[S11] Yu Y, Li J, Luo J, Kang Z, Jia C, Liu Z, Huang W, Chen Q, Deng P, Shen Y, Tian X, Mo-decorated cobalt phosphide nanoarrays as bifunctional electrocatalysts for efficient overall water/seawater splitting. *Mater. Today Nano*, 2022, 18, 100216.

[S12] Yu L, Xiao J, Huang C, Zhou J, Qiu M, Yu Y, Ren Z, Chu C W, Yu C J, High-performance seawater oxidation by a homogeneous multmetallic layered double hydroxide electrocatalyst. *Proc. Natl. Acad. Sci. U.S.A.*, 2022, 119, 2202382119.